

Mono-substituted silicotungstates as active catalysts for sustainable oxidations: homo- and heterogeneous performance†

Cite this: DOI: 10.1039/c3nj00243h

Salette S. Balula,^{*a} Luís Cunha-Silva,^a Isabel C. M. S. Santos,^b Ana C. Estrada,^c A. C. Fernandes,^d José A. S. Cavaleiro,^b João Pires,^d Cristina Freire^a and Ana M. V. Cavaleiro^b

A series of tetrabutylammonium (TBA) salts of the transition metal mono-substituted silicotungstates $[\text{SiW}_{11}\text{M}(\text{H}_2\text{O})\text{O}_{39}]^{n-}$, $\text{M} = \text{Co}^{\text{II}}, \text{Fe}^{\text{III}}, \text{Mn}^{\text{III}}, (\text{SiW}_{11}\text{M})$ were explored as homogeneous catalysts for the oxidation of geraniol and styrene with H_2O_2 . The most active homogeneous catalysts (SiW_{11}Co and SiW_{11}Fe) were immobilized onto an amine-functionalized SBA-15 (aptesSBA-15) and the resulting composites were characterized using several techniques (FT-IR, FT-Raman, UV-Vis/DRS, elemental analysis, powder XRD, SEM and N_2 adsorption-desorption isotherms). The catalytic performance of the new composites $\text{SiW}_{11}\text{Co@aptesSBA-15}$ and $\text{SiW}_{11}\text{Fe@aptesSBA-15}$ was investigated under similar experimental conditions to those used for homogeneous counterparts. 2,3-Epoxygeraniol and benzaldehyde were the main products obtained from geraniol and styrene oxidation, respectively, for all the catalysts. SiW_{11}Co and $\text{SiW}_{11}\text{Co@aptesSBA-15}$ showed to be the most active catalysts for the oxidation of geraniol and styrene. The recyclability of the composite $\text{SiW}_{11}\text{Co@aptesSBA-15}$ was investigated for three reaction cycles. The stability of the composites was confirmed using several techniques after catalytic cycles.

Received (in NJBRA)

5th March 2013,

Accepted 16th April 2013

DOI: 10.1039/c3nj00243h

www.rsc.org/njc

1. Introduction

The search of new, efficient and selective catalytic systems capable of oxidising organic compounds under sustainable conditions is a research area of high interest. Catalytic epoxidation of alkenes and monoterpenes has attracted much attention for organic syntheses, since their products are among the most useful synthetic intermediates, as well as in industry processes. Catalytic function of polyoxometalates (POMs) has been a remarkable research target due to their acidic and redox properties, which can be controlled at atomic or molecular levels.^{1–3} In particular,

transition metal substituted POMs are attractive as catalysts for oxidative reactions because they can be viewed as reactive low valent transition metal centers complexed by inorganic oxometalate ligands, which have high capacity as oxygen transfer agents.^{1,3–6}

Besides the dioxygen, hydrogen peroxide is one of the most attractive oxidants because it is environmentally clean and easily handled,⁷ and the interest in these oxidants has been rising in polyoxometalate catalysis. Among the Keggin type silicotungstates, di-lacunary and di-metal-substituted anions have been reported as active catalysts for the oxidation of several hydrocarbons with H_2O_2 . In particular, the divacant $[\gamma\text{-SiW}_{10}\text{O}_{36}]^{8-}$ ion^{3,8–14} and several dimetal-substituted $[\gamma\text{-SiW}_{10}\text{M}_2\text{O}_{36}]^{n-}$ anions ($\text{M} = \text{Fe}, \text{Mn}, \text{Ti}, \text{Cu}$)^{15–21} have been the most investigated. Less attention has been paid to the catalytic performance of mono-substituted silicotungstates as oxidative catalysts. To the best of our knowledge, only a few publications have addressed this family of POMs using oxygen as oxidant. The first work was published in 2000 and consists of the oxidation of *p*-xylene using $[\text{SiW}_{11}\text{M}(\text{H}_2\text{O})\text{O}_{39}]^{6-}$ with $\text{M} = \text{Co}^{\text{II}}$ and Cu^{II} .²² Later, Yamaguchi and Mizuno published the oxidation of different alkanes and alcohols using the ruthenium substituted anion $[\text{SiW}_{11}\text{Ru}(\text{H}_2\text{O})\text{O}_{39}]^{5-}$ as active catalyst with molecular oxygen.²³ Kortz *et al.* described the aerobic oxidation of cyclohexane by $[\text{SiW}_{11}\text{Fe}(\text{H}_2\text{O})\text{O}_{39}]^{5-}$ using microwave radiation.²⁴

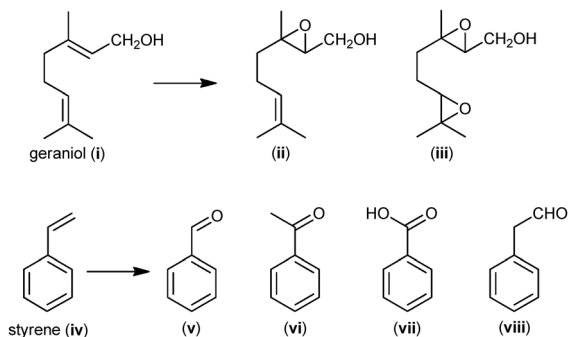
^a REQUIMTE, Departamento de Química e Bioquímica, Faculdade de Ciências, Universidade do Porto, 4169-007 Porto, Portugal. E-mail: sbalula@fc.up.pt; Fax: +351 220402659; Tel: +351 220402576

^b Departamento de Química, QOPNA, Universidade de Aveiro, 3810-193 Aveiro, Portugal

^c Departamento de Química, CICECO, Universidade de Aveiro, 3810-193 Aveiro, Portugal

^d Departamento de Química e Bioquímica, CQB, Faculdade de Ciências, Universidade de Lisboa, Campo Grande C8, 1749-016 Lisboa, Portugal

† Electronic supplementary information (ESI) available: Additional crystal structure figures; FT-IR, FT-Raman and diffuse reflectance spectra; N_2 isotherms and SEM images. CSD 424106. For ESI and crystallographic data in CIF or other electronic format see DOI: 10.1039/c3nj00243h



Scheme 1

Using H_2O_2 as oxidant, we have performed a few studies for the oxidation of different alkane substrates, using the mono-substituted silicotungstates as active homogeneous catalysts.^{25–28} Some reports indicated that monosubstituted silicotungstates were inactive in catalytic epoxidations with H_2O_2 in biphasic systems (under the conditions of the Ishii–Venturello epoxidation system).²⁹ The lack of interest in the use of these silicotungstates in catalytic epoxidations with H_2O_2 may possibly stem from these previous results. The work presented in this paper demonstrates that it is worthwhile to perform catalytic studies using these catalysts.

The difficulty of active homogeneous catalyst recyclability and the product separation are present concerns that can be solved by the immobilization of the active species on solid supports. Many supports have been referred to previously in studies with POMs, but only a few published studies report the immobilization of POMs on SBA-15^{30–34} and only two publications report the immobilization of silicotungstates on this support.^{32,33}

In the present work, we describe the oxidation of geraniol (i) and styrene (iv) by H_2O_2 in MeCN (Scheme 1), catalysed by various transition metal mono-substituted $[\text{SiW}_{11}\text{M}(\text{H}_2\text{O})_{39}]^{m-}$, $\text{M} = \text{Mn}^{\text{III}}$, Fe^{III} , Co^{II} (SiW_{11}M). Furthermore, the most active homogeneous silicotungstates were immobilized onto amine-modified SBA-15 (aptesSBA-15) support material. The catalytic activity, the recycle capability and the stability of $\text{SiW}_{11}\text{M}@aptes\text{SBA-15}$ ($\text{M} = \text{Co}$ and Fe) were investigated.

2. Experimental

2.1. Materials and methods

Geraniol, styrene and (3-aminopropyl)triethoxysilane (aptes) were purchased from Aldrich and used without further purification. Acetonitrile (99.5% Panreac), 30% H_2O_2 (Aldrich) and other reagents were used as received.

Metal analysis for K, W, Fe, Mn, Co was performed using ICP spectrometry (University of Aveiro) and C, H, N elemental analysis was performed on a Leco CHNS-932. Hydration water contents were determined using thermogravimetric analysis on a TGA-50 Shimadzu thermobalance.

Fourier transform infrared (FT-IR) absorption spectra were obtained on a Mattson 7000 FT-IR spectrometer, using KBr pellets. Spectra were collected in the range $400\text{--}4000\text{ cm}^{-1}$, using a resolution of 4 cm^{-1} and 32 scans. Fourier transform

Raman (FT-Raman) spectra were recorded on a RFS-100 Bruker FT-spectrometer, equipped with a Nd:YAG laser with excitation wavelength of 1064 nm, and laser power set to 200 mW.

Diffuse reflectance spectra (UV-Vis/DRS) were registered on a Jasco V-560 spectrophotometer, using MgO as reference.

Nitrogen (Air Liquide, 99.999%) physisorption experiments were made at $-196\text{ }^\circ\text{C}$ using a volumetric apparatus (NOVA 2200e, surface area and pore size analyzer). For every experiment, about 50 mg of the sample was degassed for 2.5 h at $150\text{ }^\circ\text{C}$ at a pressure lower than 0.133 Pa.

Scanning electron microscopy (SEM) analysis was performed at “CEMUP – Centro de Materiais da Universidade do Porto” (Porto, Portugal), using a high resolution environmental scanning electron microscope (FEI Quanta 400 FEG ESEM). The samples were analysed as powders.

Powder XRD analyses were made in a Philips Analytical PW 3050/60 X’Pert PRO ($\theta/2\theta$) diffractometer equipped with an X’Celerator detector and with automatic data acquisition (X’Pert Data Collector v2.0b software) using a monochromatized $\text{CuK}\alpha$ radiation ($\lambda = 1.5406\text{ \AA}$). Diffractograms were obtained by continuous scanning from 0.33° to $5.0^\circ 2\theta$, with a step size of $0.033^\circ 2\theta$, and 40 kV and 40 mA in the X-ray tube.

The GC-MS analyses were performed on Finnigan Trace GC-MS (Thermo Quest CE instruments) using helium as the carrier gas (35 cm s^{-1}); GC-FID was performed using a Varian Star 3400CX chromatograph to monitor homogeneous reactions, and a Varian CP-3380 to follow the heterogeneous reactions. The hydrogen was used as the carrier gas (55 cm s^{-1}) for the first case and for the second helium was utilized. In both cases, fused silica Supelco capillary columns SPB-5 ($30\text{ m} \times 0.25\text{ mm i.d.}$; $25\text{ }\mu\text{m}$ film thickness) were employed.

2.2. Synthesis of silicotungstates

The potassium salts of mono-substituted silicotungstates were prepared from the commercial silicotungstic acid at pH 6 in the presence of the transition metal to be incorporated in the silicotungstate framework. The detailed procedures are well described in the literature: $\text{K}_5[\text{SiW}_{11}\text{Fe}^{\text{III}}(\text{H}_2\text{O})_{39}] \cdot 10\text{H}_2\text{O}$ ($\text{KSiW}_{11}\text{Fe}$), $\text{K}_5[\text{SiW}_{11}\text{Mn}^{\text{III}}(\text{H}_2\text{O})_{39}] \cdot 7\text{H}_2\text{O}$ ($\text{KSiW}_{11}\text{Mn}$) and $\text{K}_4\text{H}_2[\text{SiW}_{11}\text{Co}^{\text{II}}(\text{H}_2\text{O})_{39}] \cdot 22\text{H}_2\text{O}$ ($\text{KSiW}_{11}\text{Co}$).^{35–38} The tetrabutylammonium (TBA) salts were obtained from the respective potassium salts using a procedure reported previously.^{39,40} An aqueous solution of the previously prepared potassium silicotungstate and a solution of TBABr in 1,2-dichloroethane were mixed and vigorously stirred. The organic phase was collected and the 1,2-dichloroethane removed by evaporation. The so-obtained oil was then dissolved in acetonitrile and the resultant tetrabutylammonium compound was precipitated by the addition of the minimum amount of water. All solids were characterised using elemental and thermal analysis, FT-IR and FT-Raman and electronic absorption spectroscopy (solution and solid). The results were in agreement with those previously published:^{35–38,40} $\text{TBA}_4\text{H}[\text{SiW}_{11}\text{Fe}^{\text{III}}(\text{H}_2\text{O})_{39}]$ ($\text{TBASiW}_{11}\text{Fe}$), $\text{TBA}_4\text{H}[\text{SiW}_{11}\text{Mn}^{\text{III}}(\text{H}_2\text{O})_{39}]$ ($\text{TBASiW}_{11}\text{Mn}$), and $\text{TBA}_4\text{H}_2[\text{SiW}_{11}\text{Co}^{\text{II}}(\text{H}_2\text{O})_{39}] \cdot \text{H}_2\text{O}$ ($\text{TBASiW}_{11}\text{Co}$). The only exception was the $\text{KSiW}_{11}\text{Co}$ compound, $\text{K}_4\text{H}_2[\text{SiW}_{11}\text{CoH}_2\text{O}_{40}] \cdot 22\text{H}_2\text{O}$,

that was obtained with a different molecular formula (four K^+ were found instead of six). Anal (wt%). Found: K, 5.21; W, 61.0; Co, 1.70; H_2O , 12.8% calcd: K, 4.73; W, 61.19; Co, 1.78; H_2O , 12.1%. FT-IR (cm^{-1}) 999 (m), 965 (vs), 914 (vs), 815 (vs, sh), 719 (s), 540 (vs).

2.3. Single crystal X-ray analysis

Crystalline material of $KSiW_{11}Co$ was harvested from the crystallization vial, immediately immersed in viscous oil, and a suitable single-crystal was selected and mounted on the CryoLoop.⁴¹ Data were collected on a Bruker X8 Kappa APEX II charge-coupled device (CCD) area-detector diffractometer (Mo K_{α} graphite-monochromated radiation, $\lambda = 0.71073 \text{ \AA}$) controlled by the APEX2 software package,⁴² and equipped with an Oxford Cryo-systems Series 700 cryostream controlled with a Cryopad interface.⁴³ Images were processed using SAINT+,⁴⁴ and data were corrected for absorption using the multi-scan semi-empirical method implemented in SADABS.⁴⁵ The structure was solved using the direct methods implemented in SHELXS-97,^{46,47} allowing the immediate location of most of the heaviest atoms, and all the remaining non-H atoms were located from difference Fourier maps calculated from successive full-matrix least squares refinement cycles on F^2 using SHELXL-97.^{46,48} All non H-atoms were successfully refined using anisotropic displacement parameters. Four K^+ cations for each silicotungstate anion were directly located from difference Fourier maps, thus the charge of the silicotungstate is then supposedly compensated by the presence of H-atoms bound to the anion. Nevertheless, these charge-balancing H-atoms and those belonging to the water molecules of crystallization could not be located from difference Fourier maps or even placed in calculated positions. However, all these H-atoms were added to the empirical formula.

Crystal data for $KSiW_{11}Co$: $K_4H_2[SiW_{11}CoH_2O_{40}] \cdot 22H_2O$, $M = 3306.15$, tetragonal, space group $P4/mnc$, $a = 14.1182(7) \text{ \AA}$, $b = 14.1182(7) \text{ \AA}$, $c = 12.4604(11) \text{ \AA}$, $\alpha = \beta = \gamma = 90.00^\circ$, $V = 2483.7(3) \text{ \AA}^3$, $T = 150(2) \text{ K}$, $Z = 2$, $\mu = 26.184 \text{ mm}^{-1}$, 11494 reflections measured, 1333 independent reflections ($R_{int} = 0.0486$). The final R_1 values were 0.0382 [$I > 2\sigma(I)$]. The final $wR(F^2)$ values were 0.0952 [$I > 2\sigma(I)$]. The final R_1 values were 0.0409 (all data). The final $wR(F^2)$ values were 0.0971 (all data). Crystallographic information (excluding structure factors) can be obtained free of charge *via* http://www.fiz-karlsruhe.de/obtaining_crystal_structure_data.html or from the Inorganic Crystal Structure Database (ICSD, FIZ Karlsruhe, Hermann-von-Helmholtz-Platz 1, Eggenstein-Leopoldshafen, 76344, Germany; phone: +49 7247808555, fax: +49 7247808259; e-mail: cysdata@fiz-karlsruhe.de), on quoting the depository numbers CSD-424106.

2.4. Immobilization of silicotungstates onto SBA-15

SBA-15 was obtained following a procedure adapted from the literature, using the block copolymer Pluronic P123 and tetraethyl orthosilicate (TEOS) under acidic conditions. The template was removed by calcination at 550°C .⁴⁹ The surface of SBA-15 was modified by post-grafting methodology with (3-aminopropyl)-triethoxysilane (aPTes), using a procedure reported previously.⁵⁰ The dried support was refluxed for 24 h in dry toluene with aPTes

under argon. The obtained solid was characterized using C,H,N elemental analysis, FT-IR, FT-Raman spectroscopy, powder XRD, analysis of N_2 adsorption isotherms and SEM analysis. The resulting aPTesSBA-15 contained 1.2 mmol of NH_2 per 1 gram of material. The immobilization of silicotungstates was performed by stirring the mixture of 0.5 g of amine-modified SBA-15 in 50 mL of water with 0.4 mmol of $KSiW_{11}Co$ and $KSiW_{11}Fe$, for 24 h at room temperature. The resulting materials were filtered and washed with water until the filtrate did not show any POM (monitored using UV-Vis spectroscopy). Finally, the solids were dried under vacuum for several hours at 100°C . The obtained composites were characterized using the techniques mentioned above as well as diffuse reflectance spectroscopy and ICP analysis. The loading of silicotungstates achieved was 110 μmol (22 wt% of W) of $SiW_{11}Co$ for $SiW_{11}Co@apt\text{esSBA-15}$ and 89 μmol (18 wt% of W) of $SiW_{11}Fe$ for $SiW_{11}Fe@apt\text{esSBA-15}$, per gram of material.

2.5. Oxidation reactions

The oxidation reactions of geraniol (**i**) and styrene (**iv**) (Scheme 1) were carried out in MeCN, in a borosilicate 10 mL reaction vessel, with addition of aqueous H_2O_2 (30 wt%), in the presence of TBA salts of the silicotungstate ($SiW_{11}M$, $M = Fe^{III}$, Mn^{III} , Co^{II}) or of the silicotungstate composites (27 mg of $SiW_{11}Co@apt\text{esSBA-15}$ and 34 mg of $SiW_{11}Fe@apt\text{esSBA-15}$). In the oxidation of (**i**) the reaction was performed at room temperature and protected from light. The oxidative reactions of (**iv**) were carried out at 80°C . In a typical experiment, MeCN (1.5 mL) was added to the substrate (1 mmol) and the catalyst (3 μmol) was placed in the reaction vessel and stirred. H_2O_2 was added to the reaction mixture, 500 μl (4.5 mmol) for the oxidation of (**i**) and (**iv**). The reactions were followed by GC analysis and stopped when a complete conversion of the substrate was observed or when the product yields remained constant after two successive GC analysis. At regular intervals, an aliquot was taken directly from the reaction mixture using a microsyringe, diluted in MeCN, centrifuged (if necessary) and injected into the GC or GC-MS equipment for analysis of starting materials and products. The reaction products reported here were identified as described elsewhere.^{51,52} The heterogeneous catalyst was filtered off at the end of reactions, washed with MeCN several times to remove the remaining substrate, reaction products and oxidant. The recovered catalyst was dried at room temperature overnight and reused in a new reaction under identical experimental conditions, with readjustment of all quantities, without changing the molar ratios and reaction concentrations. Blank reactions were performed for all substrates, confirming that no oxidation products are obtained unless the catalyst and H_2O_2 are present. Even in the presence of the support aPTesSBA-15 no oxidation products were obtained.

3. Results and discussion

3.1. Catalysts preparation and characterization

The potassium and the TBA compounds of the anions $[SiW_{11}M(H_2O)_9]^{7-}$ ($M = Mn^{III}$, Fe^{III} , Co^{II}) have been described

previously.^{35–38,40,53} Still, the compound $\text{K}_4\text{H}_2[\text{SiW}_{11}\text{Co}(\text{H}_2\text{O})\text{O}_{39}] \cdot 22\text{H}_2\text{O}$ ($\text{KSiW}_{11}\text{Co}$) was obtained in this work, instead of the more common $\text{K}_6[\text{SiW}_{11}\text{Co}(\text{H}_2\text{O})\text{O}_{39}] \cdot 13\text{H}_2\text{O}$ usually referred in the literature.³⁷ Furthermore, crystalline material of the $\text{KSiW}_{11}\text{Co}$ suitable for single-crystal X-ray diffraction (XRD) analysis could be grown. The crystal structure was determined in the tetragonal $P4/nmc$ space group (for details concerning the crystallographic data collection and refinement see Experimental section), being isostructural with related compounds such as $\text{K}_4\text{H}_2[\text{SiW}_4\text{Mo}_7\text{Ni}(\text{H}_2\text{O})\text{O}_{39}] \cdot 13(\text{H}_2\text{O})$ ⁵⁴ and $\text{K}_4\text{H}_2[\text{SiW}_7\text{Mo}_4\text{Co}(\text{H}_2\text{O})\text{O}_{39}] \cdot 22(\text{H}_2\text{O})$.⁵⁵ Furthermore, the comparison of the structure of $\text{K}_4\text{H}_2[\text{SiW}_{11}\text{Co}(\text{H}_2\text{O})\text{O}_{39}] \cdot 22\text{H}_2\text{O}$ with that of $\text{K}_6[\text{SiW}_{11}\text{Co}(\text{H}_2\text{O})\text{O}_{39}] \cdot 13\text{H}_2\text{O}$ based on the powder XRD patterns reveals substantial similarities.^{56,57} The structure is build up of K^+ cations, Keggin type $[\text{SiW}_{11}\text{Co}(\text{H}_2\text{O})\text{O}_{39}]^{6-}$ anions (Fig. S1 in the ESI†) and hydration water molecules (Fig. S2, ESI†). As a consequence of the $4/m$ symmetry, each oxygen atom of the central SiO_4 group of the polyoxoanion is disordered over two half-occupied sites, corresponding to a 90° relative rotation of the Keggin anions. Furthermore, as a consequence of the high symmetry of this structure and the molecular disorder it is not possible to differentiate the Co^{II} centre from the eleven W^{VI} centres, thus the Co and eleven W atoms were equally distributed and refined in the twelve metallic positions of the polyoxoanion (Fig. S1, ESI†).

SBA-15 was chosen as support material to prepare the heterogeneous catalysts due to its large surface area, easy surface modification with functional groups, high stability and low toxicity. This support was functionalized by reaction with the organosilane aptses in a post-synthesis step,⁵⁰ and the silicotungstate SiW_{11}Fe and SiW_{11}Co were immobilized on the amine-functionalized SBA-15 (aptsesSBA-15) through a procedure previously used to prepare supported phosphotungstates.³⁴ The amount of amine groups on the surface of the material was determined by elemental analysis of C and N (1.2 mmol of NH_2 per 1 gram of material) and the amount of silicotungstate by the analysis of tungsten (0.11 mmol g^{-1} of SiW_{11}Co , 0.089 mmol g^{-1} of SiW_{11}Fe). Furthermore, the metal analysis of W, Co and Fe suggests that no degradation of the structure of the transition metal substituted silicotungstate occurred since the molar ratio of W/Co or W/Fe is approximately 11 in both cases. The immobilization of mono-substituted silicotungstates SiW_{11}Fe and SiW_{11}Co can occur by the coordination of the transition metal (Fe^{III} and Co^{II}) with the amine group present on the support material, as suggested before in the literature for other mono-substituted polyoxometalates immobilized onto various amine-functionalized silica supports.^{31,58,59} Other hypothesis is the electrostatic interaction with protonated amine groups.⁶⁰

The presence of immobilized silicotungstates and the stability of the aptsesSBA-15 material after immobilization were established using various spectroscopic methods, including UV-Vis/DRS, FT-IR and FT-Raman. Fig. 1 and Fig. S4 in ESI† present the FT-IR spectra of the immobilized silicotungstates and the support aptsesSBA-15. The stronger bands in the region of $400\text{--}1100\text{ cm}^{-1}$ are attributed to the SBA-15 $\nu_{\text{as}}(\text{Si-O-Si})$, $\nu_{\text{s}}(\text{Si-O-Si})$ and $\delta(\text{O-Si-O})$ which overlap the characteristic bands of the silicotungstates (Fig. S3, ESI†). In the region of $1500\text{--}1580\text{ cm}^{-1}$ two weak bands assigned to the NH_2 groups can be observed, which confirms the incorporation of

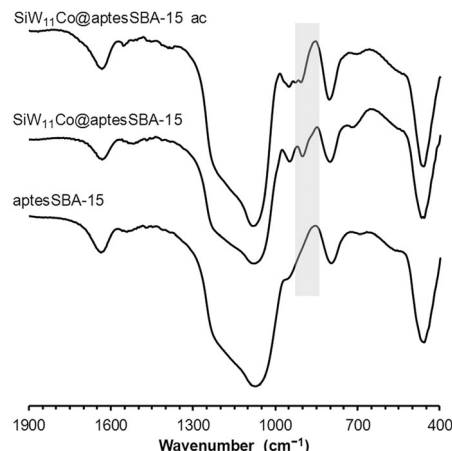


Fig. 1 FT-IR spectra of support aptsesSBA-15 and silicotungstate composites in the wavenumber region between 400 and 1900 cm^{-1} . Name of samples with ac corresponds to recovered samples after catalyzing the styrene oxidation reaction.

amine groups on the aptsesSBA-15 material.⁶¹ Comparing the spectrum of the support aptsesSBA-15 with the spectra of $\text{SiW}_{11}\text{Fe@aptsesSBA-15}$ and $\text{SiW}_{11}\text{Co@aptsesSBA-15}$ it is possible to find additional bands that indicate the presence of the immobilized silicotungstate on the support. One of the characteristic bands that can be identified in the spectra of composite materials appears at $ca. 920\text{ cm}^{-1}$ and is attributed to $\nu_{\text{as}}(\text{W-O-W})$ and $\nu_{\text{as}}(\text{Si-O})$ that cannot be distinguished by their wavelength proximity (Fig. 1). The infrared spectra of isolated silicotungstates SiW_{11}Co and SiW_{11}Fe are presented in Fig. S3, ESI†.

The FT-Raman spectra of the immobilized silicotungstates are more elucidative than the FT-IR data because the silica support does not show any band on the region of the Keggin silicotungstates. Similar patterns are found for $\text{SiW}_{11}\text{Fe@aptsesSBA-15}$ and $\text{SiW}_{11}\text{Co@aptsesSBA-15}$ when compared with those of the TBA salts of SiW_{11}Fe and SiW_{11}Co and their characteristic bands are seen without any interference due to the support (Fig. 2 and Fig. S5, ESI†). The spectra of SiW_{11}Fe and SiW_{11}Co show a strong band

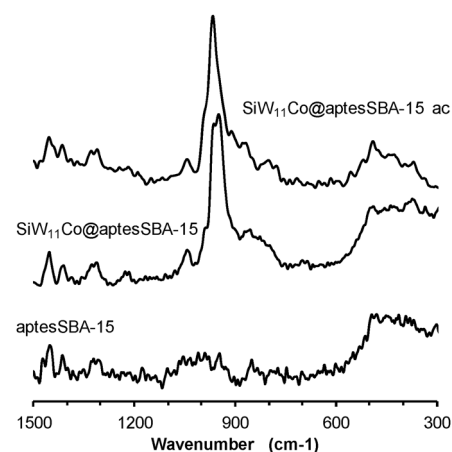


Fig. 2 FT-Raman spectra of aptsesSBA-15 and silicotungstate composites in the wavenumber region between 300 and 1500 cm^{-1} . Name of samples with ac corresponds to recovered samples after catalyzing the styrene oxidation reaction.

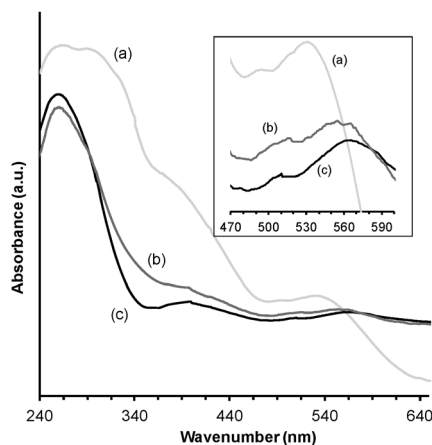


Fig. 3 Diffuse reflectance electronic spectra: (a) TBASiW₁₁Co, (b) SiW₁₁Co@aptesSBA-15 and (c) SiW₁₁Co@aptesSBA-15-ac, where ac means after catalyzing the styrene oxidation reaction.

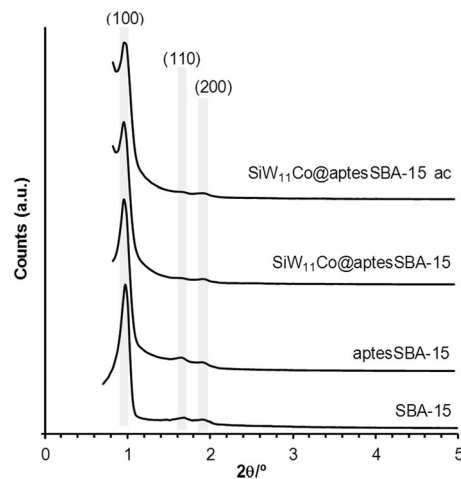


Fig. 4 Powder X-ray diffraction patterns for the indicated samples.

near 1000–970 cm⁻¹ attributed to $\nu_s(W-O)$ that corresponds to the bond between tungsten and the terminal oxygen.^{39,62} This band is slightly shifted to lower wavenumbers when silicotungstates are supported onto aptesSBA-15 (Fig. S5, ESI[†]).

The UV-Vis/DRS spectra of SiW₁₁Co@aptesSBA-15 and SiW₁₁Fe@aptesSBA-15 reveal a band with λ_{max} ca. 270 nm, which is attributed to oxygen-to-tungsten charge transfer from W–O–W bonds of silicotungstates (Fig. 3 and Fig. S6, ESI[†]).⁶³ Furthermore, the spectra of SiW₁₁Co and the composite SiW₁₁Co@aptesSBA-15 can be compared to evaluate possible alterations of Co^{II} coordination environment after immobilization. The spectrum of SiW₁₁Co shows one splitted band with λ_{max} ca. 540 nm that corresponds to d–d electronic transition.³⁷ However, the same band is enlarged, with λ_{max} shifted to higher wavelength (ca. 570 nm) when the same compound was immobilized on aptesSBA-15, which may indicate an alteration of the coordination sphere of Co^{II} (Fig. 3). A shift of the d–d band from Co^{II} incorporated into phosphotungstate structures was observed before when the compound was immobilized on amino-modified mesoporous silica.^{31,58} The UV-Vis/DRS spectra of SiW₁₁Fe and SiW₁₁Fe@aptesSBA-15 (Fig. S6, ESI[†]) show charge transfer bands (O → W and O → Fe).

The results obtained from the analysis of FT-IR, FT-Raman and UV-Vis/DRS comparing the isolated silicotungstates and the supported silicotungstates suggest that SiW₁₁Fe and SiW₁₁Co are effectively immobilized on the aptesSBA-15 and no degradation of silicotungstates structure occurred.

Powder XRD patterns are depicted in Fig. 4. The strong reflection characteristic of SBA-15 type materials⁶⁴ is displayed and, as overall, the peaks can be indexed on a hexagonal lattice as reflections (100) (110) and (210). The results confirm the integrity of the SBA-15 after the various steps of functionalization and supporting the POMs.

The nitrogen adsorption–desorption isotherms at –196 °C present the usual shape for SBA-15 type of materials,⁶⁵ and can be classified as Type IV with H1 hysteresis loop (Fig. 5).⁶⁶ The adsorbed amounts are reduced upon the surface functionalization

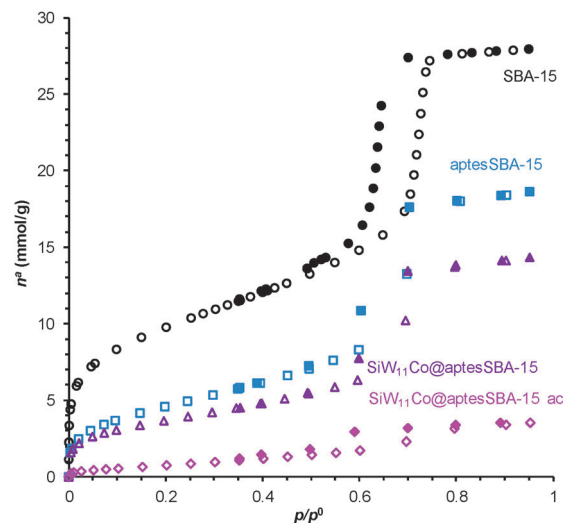


Fig. 5 Nitrogen adsorption–desorption isotherms at –196 °C for the initial and modified SBA-15 samples. Name of samples with ac corresponds to recovered samples after catalyzing the styrene oxidation reaction.

with aptes and so the specific surface area is lowered to near 50% of the initial value (Table 1). Nevertheless, after grafting the silicotungstates in the aptesSBA-15 sample, only a small reduction in the surface area and porous volume is noticed, meaning that a considerable amount of porous volume (near 0.5 cm³ g⁻¹) is still available in the prepared catalysts.

The pore size distributions (Fig. S7, ESI[†]) were obtained using the DFT method and reveal a shift for lowest pore sizes for the materials upon functionalization/grafting and also some

Table 1 Textural properties of the solid support and heterogeneous catalysts

	A_{BET} (m ² g ⁻¹)	Total pore volume (cm ³ g ⁻¹)
SBA-15	763	0.976
aptesSBA-15	380	0.650
SiW ₁₁ Co@aptesSBA-15	298	0.497
SiW ₁₁ Co@aptesSBA-15 ac	62	0.122

broadening of the distributions. In general, the results for the pore size distributions are compatible with the presence of the silicotungstates mainly inside the porous structure of the SBA-15 material.

3.2. Homogeneous catalysis

The oxidation of geraniol and styrene was carried out in homogeneous phase using H_2O_2 as oxidant and MeCN as solvent, in the presence of catalytic amounts of TBA salts of silicotungstates SiW_{11}M ($\text{M} = \text{Mn}^{\text{III}}$, Fe^{III} and Co^{II}). All the silicotungstates could catalyse the reactions studied (Fig. 6). In the absence of a catalyst the conversion never exceeded 7% after 24 h of reaction.

The main product obtained from the oxidation of geraniol (i) with H_2O_2 at room temperature was 2,3-epoxygeraniol (ii, Scheme 1) in the presence of all catalysts, with selectivity always higher than 90%, indicating the highly chemoselective nature of the reactions. A small amount of diepoxide (iii) was found after 6 h of reaction in the presence of all studied catalysts (Table 2). The best catalytic performance was observed for SiW_{11}Co which attained 95% of conversion and 100% of selectivity after 30 minutes of reaction. After 6 h of reaction, almost complete conversion of geraniol was achieved in the presence of all catalysts. The efficiency of the usage of H_2O_2 was analyzed for the oxidation of this substrate catalysed by SiW_{11}Co . Fig. S8 in ESI† display the comparison of the amount

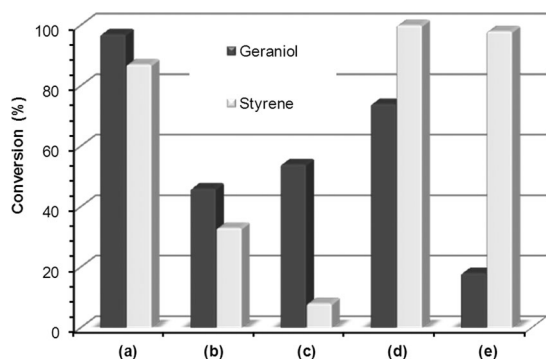


Fig. 6 Conversion data obtained for the oxidation of different substrates after 1 h of reaction when catalysed by homogeneous silicotungstates: (a) SiW_{11}Co , (b) SiW_{11}Fe , (c) SiW_{11}Mn ; and after 24 h when catalysed by the composites (d) $\text{SiW}_{11}\text{Co}@ \text{aptesSBA-15}$ and (e) $\text{SiW}_{11}\text{Fe}@ \text{aptesSBA-15}$. Reaction conditions: 3 μmol of silicotungstate, 1 mmol substrate, 4.5 mmol H_2O_2 , 1.5 mL MeCN, 80 $^\circ\text{C}$ (room temperature and light protection in the presence of geraniol).

Table 2 Conversion (%) and selectivity (%) for the oxidation reaction of geraniol with H_2O_2 using homogeneous silicotungstate catalysts^a

Catalyst	Conv. 1 h (select.) ^b	Conv. 6 h (select.) ^b
SiW_{11}Co	97 (95)	97 (94)
SiW_{11}Fe	46 (94)	99 (96)
SiW_{11}Mn	54 (98)	99 (95)

^a Reaction conditions: 1 mmol of geraniol, 4.5 mmol H_2O_2 , 3 μmol of silicotungstate, 1.5 mL MeCN, room temperature and light protection.

^b Based on the amount of consumed substrates; corresponding to 2,3-epoxygeraniol.

of geraniol oxidized and the amount of H_2O_2 consumed during 6 h of reaction. The efficiency of H_2O_2 usage was observed to decrease with reaction time and 94, 80 and 52% were obtained after 30 min, 1 h and 6 h, respectively.

Few studies have been published for the oxidation of geraniol catalysed by Keggin type POMs and most of them have been performed using homogeneous systems.^{67–69} Recently, some metal mono-substituted phosphotungstates and borotungstates were used to oxidise selectively geraniol to 2,3-epoxygeraniol under similar experimental conditions used in this work.^{34,67,68} However, in the presence of SiW_{11}Co higher substrate conversion was achieved in this work for less reaction time.

The oxidation of styrene catalysed by silicotungstates yielded benzaldehyde (v) as the main product. Benzaldehyde is the only product detected during the first 30 min of reaction in the presence of all catalysts; however, its selectivity decreases with the increase of the reaction time because other products such as acetophenone (vi), phenylacetaldehyde (viii) and benzoic acid (vii) are also produced (Scheme 1). Table 3 shows the product distribution and the catalytic performance obtained for styrene oxidation after 6 and 24 h in the presence of different silicotungstates. The best catalytic performance was found for SiW_{11}Co where after 6 h a complete conversion was obtained. This catalyst showed a fast activity since the first minute of reaction and after 30 min a conversion of 62% was achieved with 80% of selectivity to benzaldehyde. At this stage phenylacetaldehyde, acetophenone and benzoic acid are also produced. The SiW_{11}Co has been studied before as a homogeneous catalyst for styrene oxidation under different experimental conditions; however, better catalytic results were found in our work when we increased the ratio substrate/oxidant to 1:4.5 and when the volume of MeCN was decreased to 1.5 mL.³³ Using SiW_{11}Fe as catalyst a complete conversion of styrene was achieved; however, larger H_2O_2 excess and long reaction time were required.⁷⁰

The oxidation of styrene to benzaldehyde with H_2O_2 catalyzed by polyoxotungstates and peroxophosphotungstates is already well documented in the literature.^{33,71–73} The mechanism proceeds initially by the interaction of H_2O_2 with the POM, generating active species which may be hydroperoxo or bridging

Table 3 Data for the oxidation reaction of styrene in the presence of different catalysts^{ab}

Catalyst	Conv. (%)	Select. ^c (%)			
		v	vi	vii	viii
No catalyst	≈ 0	—	—	—	—
SiW_{11}Co	99	75	7	7	11
SiW_{11}Fe	68 (100)	74 (65)	10 (19)	9 (7)	7 (9)
SiW_{11}Mn	19 (22)	58 (55)	(27)	(9)	42 (9)
$\text{SiW}_{11}\text{Co}@ \text{aptesSBA-15}$	58 (100)	100 (75)	(25)	—	—
$\text{SiW}_{11}\text{Fe}@ \text{aptesSBA-15}$	41 (98)	100 (52)	(48)	—	—

^a Conversion and selectivity data at 6 h of reaction, except values in parentheses, obtained after 24 h of reaction. ^b Reaction conditions: 1 mmol of styrene, 4.5 mmol H_2O_2 , 3 μmol of silicotungstate or the amount of composite containing 3 μmol of silicotungstate, 1.5 mL MeCN and 80 $^\circ\text{C}$. ^c Selectivity for the various products obtained from styrene oxidation assigned in Scheme 1.

peroxy species. Afterwards, styrene is bonded with one of the metal-peroxy bonds to produce a peroxometalloycycle and in the next step styrene oxide is formed. A further nucleophilic attack of H_2O_2 on the styrene oxide originates benzaldehyde.^{33,72} The phenylacetaldehyde is possibly formed through isomerisation of styrene oxide, while the formation of benzoic acid from benzaldehyde is a simple oxidation.⁷⁴

3.3. Heterogeneous catalysis and recyclability

The catalytic performance of $\text{SiW}_{11}\text{Co}@aptes\text{SBA-15}$ and $\text{SiW}_{11}\text{Fe}@aptes\text{SBA-15}$ was evaluated for the oxidation of geraniol and styrene under the same experimental conditions used for the homogeneous catalytic systems (oxidant 30% H_2O_2 and MeCN as solvent). Also for the heterogeneous catalytic systems the cobalt based catalyst ($\text{SiW}_{11}\text{Co}@aptes\text{SBA-15}$) was more active than the $\text{SiW}_{11}\text{Fe}@aptes\text{SBA-15}$ (Fig. 6). Comparing the performance of the heterogeneous catalyst with the corresponding homogeneous catalyst it is possible to notice that the first showed to be less active for the oxidation of both substrates. From the oxidation of geraniol (i) only the 2,3-epoxygeraniol (ii) was produced. The benzaldehyde (v) was the main product obtained from styrene oxidation and only acetophenone (vi) was formed as a by-product (Table 3). During the first six hours of styrene oxidation reaction a decrease of activity was observed when the heterogeneous systems were used instead of the homogeneous compounds (Fig. 7). However, after 24 h a complete conversion was attained by the homogeneous and heterogeneous catalytic systems (Fig. 7).

Many cobalt(II)-catalyzed systems for oxidation of alkenes with molecular oxygen (often involving a co-reductant, such as an aldehyde) have been reported.^{75–77} The oxidation of styrene yields usually styrene epoxide and benzaldehyde as main products, with the outcome of the reactions varying with the conditions. The oxidation of styrene by H_2O_2 , catalyzed by cobalt complexes (in homogeneous or heterogeneous conditions), is described in several papers (see, for example, ref. 78–80). With these systems, benzaldehyde is usually the major product, as found in our work. Reported yields vary between 40 and 89%,⁷⁸ showing that our results are quite good.

The solid catalysts can be easily separated by simple filtration followed by washing (with MeCN and *n*-hexane) and drying at

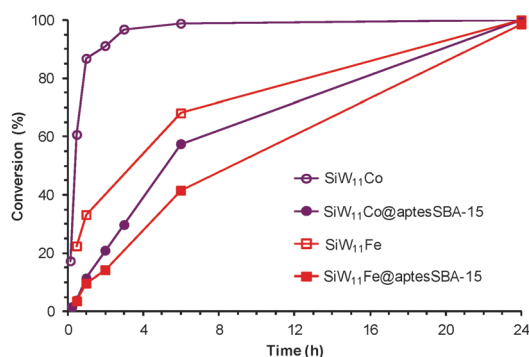


Fig. 7 Comparison of kinetic profiles for styrene oxidation of homogeneous (open symbols) and heterogeneous (solid symbols) reactions, using H_2O_2 as oxidant and MeCN as solvent.

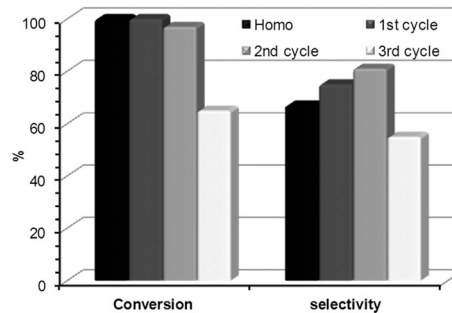


Fig. 8 Activity data obtained for the oxidation of styrene after 24 h of reaction when catalysed by the homogeneous SiW_{11}Co and by the heterogeneous $\text{SiW}_{11}\text{Co}@aptes\text{SBA-15}$ for three consecutive cycles.

room temperature to be used in a fresh reaction under identical experimental conditions. The activity of $\text{SiW}_{11}\text{Co}@aptes\text{SBA-15}$ and $\text{SiW}_{11}\text{Fe}@aptes\text{SBA-15}$ is retained from the first to the second reaction cycle; however, a decrease of activity was found in the third reaction cycle. Fig. 8 shows the reusability of the heterogeneous system $\text{SiW}_{11}\text{Co}@aptes\text{SBA-15}$ for styrene oxidation after 24 h of reaction. The selectivity for benzaldehyde is practically maintained from the first to the second reaction cycle, having only acetophenone as a by-product (Fig. 8). For the third cycle the selectivity to benzaldehyde is decreased because benzoic acid (26% of yield of (vii) in Scheme 1) is also formed.

For geraniol oxidation no conversion was found during the first 2 h of reaction for the heterogeneous systems. However, the difference of activity between homogeneous and heterogeneous systems became smaller with the reaction time, mainly for $\text{SiW}_{11}\text{Co}@aptes\text{SBA-15}$ that achieved near complete conversion after 24 h (Fig. 6). The induction period observed in the presence of the heterogeneous systems for geraniol oxidation may be due to the less accessibility of the catalyst active centre. The epoxidation of geraniol at the $\text{C}_2\text{--C}_3$ position may involve the formation of an intermediate complex between the metal centre of the catalyst, the oxidant and the substrate, that should be more difficult in the heterogeneous catalyst where the metal centre is less accessible.⁸¹

To further investigate the catalytic activity of the heterogeneous catalyst *versus* the possible homogeneous reaction with the leached active species from the support, the solid catalyst was separated from the reaction mixture by careful filtration after a certain time and the reaction was continued further with the remaining filtrate. This experiment was performed using the most active catalysts, *i.e.* $\text{SiW}_{11}\text{Co}@aptes\text{SBA-15}$ for the oxidation of styrene, where the catalyst was filtering after 1 h of reaction. Fig. 9 shows the comparison of the kinetic profile of this reaction with the case where the solid catalyst was not filtered. It can be observed a slightly increase of conversion after solid catalyst filtration what may probably indicate partial leaching of SiW_{11}Co into the filtrate albeit it was small. The W analysis of the recovered composite after catalytic use shows that 19% of the initial SiW_{11}Co loading in $\text{SiW}_{11}\text{Co}@aptes\text{SBA-15}$ was leached after three consecutive reaction cycles. According to this result, it will be important to develop in the near future new strategies to avoid the leaching of

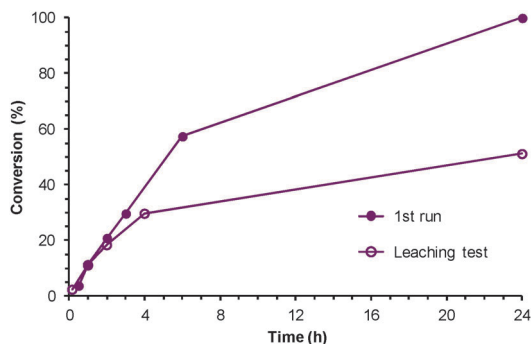


Fig. 9 Kinetic profiles for the oxidation of styrene with H_2O_2 catalysed by $\text{SiW}_{11}\text{Co@aptesSBA-15}$ (1st run) and when the same was removed after 1 h of reaction (leaching test).

active species in order to immobilize more efficiently the silicotungstates on the SBA-15 support.

3.4. Stability analysis

To investigate the stability of catalysts after reaction cycles, the materials $\text{SiW}_{11}\text{Fe@aptesSBA-15}$ and $\text{SiW}_{11}\text{Co@aptesSBA-15}$ were recovered after reaction of styrene oxidation and characterized using different techniques. The FT-IR and the FT-Raman spectra after catalytic runs reveal the same characteristic bands of silicotungstates, corresponding to $\nu_{\text{as}}(\text{W-O-W})$, $\nu_{\text{as}}(\text{Si-O})$ and $\nu_{\text{s}}(\text{W-O})$, and also the bands of the support aptesSBA-15 (Fig. 1 and 2 and Fig. S4 and S5, ESI[†]). The UV-Vis/DRS spectra of $\text{SiW}_{11}\text{Fe@aptesSBA-15}$ show the same charge transfer bands ($\text{O} \rightarrow \text{W}$, $\text{O} \rightarrow \text{Fe}$) and the spectrum of $\text{SiW}_{11}\text{Co@aptesSBA-15}$ exhibits the same d-d band of Co^{II} as observed before the catalytic runs (Fig. 3 and Fig. S6, ESI[†]). The X-ray diffractograms of $\text{SiW}_{11}\text{Co@aptesSBA-15}$ plotted after catalytic runs display the same peaks as before catalytic use, what confirm the integrity of the SBA-15 after the various catalytic reaction cycles (Fig. 4). The $\text{SiW}_{11}\text{Co@aptesSBA-15}$ composite was analysed using electron microscopy (SEM). As observed in Fig. S8, ESI[†] the morphology of the materials before and after catalytic use is similar confirming the preservation of the aptesSBA-15 structure.

The nitrogen adsorption-desorption isotherms at $-196\text{ }^\circ\text{C}$ were also performed for the composites after catalysis (Fig. 5) and it was possible to observe a reduction in the total porous volume of $\text{SiW}_{11}\text{Co@aptesSBA-15}$ after catalysis. This reduction in the specific surface area of the sample after catalysis seems to be high but the significance of this value needs to be interpreted with care. In fact, it should be emphasized that the sample was analyzed after being re-used in three catalytic cycles. At the end of the catalytic cycles it is possible that solvent molecules, as well as some reactant and product molecules, are occluded in the pore structure. In the phase of cleaning under vacuum and temperature, prior to the determination of the nitrogen adsorption isotherms, only a moderate temperature ($150\text{ }^\circ\text{C}$) could be used to avoid decomposition of the organic aptes surface groups. These experimental conditions may not allow the complete removal of the above mentioned molecules and, therefore, return a low specific surface area value.

4. Conclusions

The silicotungstates SiW_{11}M revealed to be active catalysts for the oxidation of geraniol and styrene in homogeneous ($\text{M} = \text{Co}^{\text{II}}$, Fe^{III} , Mn^{III}) and heterogeneous ($\text{M} = \text{Co}^{\text{II}}$, Fe^{III}) systems with H_2O_2 as an oxidant and MeCN as solvent. Compounds with the best homogeneous catalytic performance were immobilized onto amine-functionalized SBA-15 to prepare the heterogeneous catalysts: $\text{SiW}_{11}\text{Co@aptesSBA-15}$ and $\text{SiW}_{11}\text{Fe@aptesSBA-15}$. Comparable activities between homogeneous and heterogeneous systems were achieved after 24 h. The selectivity was higher using the heterogeneous catalysts than the homogeneous catalysts. The SiW_{11}Co and the composite $\text{SiW}_{11}\text{Co@aptesSBA-15}$ were the most active catalysts for geraniol and styrene oxidation. 2,3-Epoxygeraniol was the main product obtained from geraniol oxidation (95% and 74% of conversion were obtained using SiW_{11}Co after 30 min and $\text{SiW}_{11}\text{Co@aptesSBA-15}$ after 24 h, respectively). Benzaldehyde was the main product obtained from styrene oxidation and its selectivity was higher when the reaction was catalyzed by the heterogeneous systems (58% of conversion and 100% of selectivity for benzaldehyde were obtained after 6 h using $\text{SiW}_{11}\text{Co@aptesSBA-15}$ as catalyst).

The stability of the silicotungstate immobilized on aptesSBA-15 was verified after catalytic reactions and the integrity and recycle capability of the support were investigated. The heterogeneous character of the composites was evaluated by performing the leaching analysis and a small loss of active centers seemed to occur. When the silicotungstate composites were used in consecutive reaction cycles for styrene oxidation a moderate decrease of activity was observed from the second to the third cycle, which may be caused by the loss of an active center found after the three reaction cycles. The optimization of the catalytic systems will be carried out to minimize the leaching active species and other methodologies of SBA-15 functionalization will be investigated.

Acknowledgements

The authors acknowledge the *Fundação para a Ciência e a Tecnologia* (FCT, MEC, Portugal) for general funding (PEst-C/EQB/LA0006/2011 for Associated Laboratory REQUIMTE and PEst-C/QUI/UI0062/2011 for QOPNA) and PEst-OE/QUI/UI0612/2011 (CQB) and grant SFRH/BD/72058/2010(ACF).

References

- 1 C. L. Hill and C. M. Prosser-McCartha, *Coord. Chem. Rev.*, 1995, **143**, 407–455.
- 2 C. L. Hill, *J. Mol. Catal. A: Chem.*, 2007, **262**, 1.
- 3 N. Mizuno, K. Yamaguchi and K. Kamata, *Coord. Chem. Rev.*, 2005, **249**, 1944–1956.
- 4 I. V. Kozhevnikov, *Chem. Rev.*, 1998, **98**, 171–198.
- 5 R. Neumann, *Modern Oxidative Methods*, Wiley-VCH, Weinheim, 2004.
- 6 R. Neumann, *Progress in Inorganic Chemistry*, 1998, vol. 47, pp. 317–370.

- 7 C. W. Jones, *Applications of Hydrogen Peroxide and Derivatives*, Royal Society of Chemistry, Cambridge, 1999.
- 8 K. Kamata, K. Yonehara, Y. Sumida, K. Yamaguchi, S. Hikichi and N. Mizuno, *Science*, 2003, **300**, 964–966.
- 9 A. Yoshida, S. Hikichi and N. Mizuno, *J. Organomet. Chem.*, 2007, **692**, 455–459.
- 10 Y. Kikukawa, K. Yamaguchi and N. Mizuno, *Angew. Chem., Int. Ed.*, 2010, **49**, 6096–6100.
- 11 K. Kamata, M. Kotani, K. Yamaguchi, S. Hikichi and N. Mizuno, *Chem.–Eur. J.*, 2007, **13**, 639–648.
- 12 X. D. Yu, L. L. Xu, X. Yang, Y. N. Guo, K. X. Li, J. L. Hu, W. Li, F. Y. Ma and Y. H. Guo, *Appl. Surf. Sci.*, 2008, **254**, 4444–4451.
- 13 N. Mizuno, K. Kamata and K. Yamaguchi, *Top. Catal.*, 2010, **53**, 876–893.
- 14 N. Mizuno, S. Hikichi, K. Yamaguchi, S. Uchida, Y. Nakagawa, K. Uehara and K. Kamata, *Catal. Today*, 2006, **117**, 32–36.
- 15 N. Mizuno, M. Misono, Y. Nishiyama, Y. Seki, I. Kiyoto and C. Nozaki, *Res. Chem. Intermed.*, 2000, **26**, 193–199.
- 16 M. Bonchio, M. Carraro, A. Sartorel, G. Scorrano and U. Kortz, *J. Mol. Catal. A: Chem.*, 2006, **251**, 93–99.
- 17 Y. Goto, K. Kamata, K. Yamaguchi, K. Uehara, S. Hikichi and N. Mizuno, *Inorg. Chem.*, 2006, **45**, 2347–2356.
- 18 K. Yamaguchi, K. Kamata, S. Yamaguchi, M. Kotani and N. Mizuno, *J. Catal.*, 2008, **258**, 121–130.
- 19 K. Kamata, S. Yamaguchi, M. Kotani, K. Yamaguchi and N. Mizuno, *Angew. Chem., Int. Ed.*, 2008, **47**, 2407–2410.
- 20 Y. Nishiyama, Y. Nakagawa and N. Mizuno, *Angew. Chem., Int. Ed.*, 2001, **40**, 3639–3641.
- 21 B. Botar, Y. V. Geletii, P. Kogerler, D. G. Musaev, K. Morokuma, I. A. Weinstock and C. L. Hill, *J. Am. Chem. Soc.*, 2006, **128**, 11268–11277.
- 22 N. A. Alekar, S. Gopinathan and C. Gopinathan, *Indian J. Chem., Sect. A: Inorg., Bio-inorg., Phys., Theor. Anal. Chem.*, 2000, **39**, 439–441.
- 23 K. Yamaguchi and N. Mizuno, *New J. Chem.*, 2002, **26**, 972–974.
- 24 M. Bonchio, M. Carraro, G. Scorrano and U. Kortz, *Adv. Synth. Catal.*, 2005, **347**, 1909–1912.
- 25 M. S. S. Balula, I. C. M. S. Santos, M. M. Q. Simões, M. G. P. M. S. Neves, J. A. S. Cavaleiro and A. M. V. Cavaleiro, *J. Mol. Catal. A: Chem.*, 2004, **222**, 159–165.
- 26 A. C. Estrada, M. M. Q. Simoes, I. Santos, M. Neves, A. M. S. Silva, J. A. S. Cavaleiro and A. M. V. Cavaleiro, *Appl. Catal., A*, 2009, **366**, 275–281.
- 27 I. C. M. S. Santos, M. M. Q. Simões, M. S. S. Balula, M. G. P. M. S. Neves, J. A. S. Cavaleiro and A. M. V. Cavaleiro, *Synlett*, 2008, 1623–1626.
- 28 M. M. Q. Simões, I. C. M. S. Santos, M. S. S. Balula, J. A. F. Gamelas, A. M. V. Cavaleiro, M. G. P. M. S. Neves and J. A. S. Cavaleiro, *Catal. Today*, 2004, **91–92**, 211–214.
- 29 D. C. Duncan, R. C. Chambers, E. Hecht and C. L. Hill, *J. Am. Chem. Soc.*, 1995, **117**, 681–691.
- 30 L. F. Chen, K. Zhu, L. H. Bi, A. Suchopar, M. Reicke, G. Mathys, H. Jaensch, U. Kortz and R. M. Richards, *Inorg. Chem.*, 2007, **46**, 8457–8459.
- 31 N. V. Maksimchuk, M. S. Meigunov, Y. A. Chesalov, J. Mrowlec-Bialon, A. B. Jarzebski and O. A. Kholdeeva, *J. Catal.*, 2007, **246**, 241–248.
- 32 R. F. Zhang and C. Yang, *J. Mater. Chem.*, 2008, **18**, 2691–2703.
- 33 J. L. Hu, K. X. Li, W. Li, F. Y. Ma and Y. H. Guo, *Appl. Catal., A*, 2009, **364**, 211–220.
- 34 S. S. Balula, I. C. M. S. Santos, L. Cunha-Silva, A. P. Carvalho, J. Pires, C. Freire, J. A. S. Cavaleiro, B. Castro and A. M. V. Cavaleiro, *Catal. Today*, 2012, **203**, 95–102.
- 35 F. Zonnevijlle, C. M. Tourné and G. F. Tourné, *Inorg. Chem.*, 1982, **21**, 2751–2757.
- 36 A. Tézé and G. Hervé, *Inorganic Synthesis*, John Wiley & Sons, New York, 1990.
- 37 T. J. R. Weakley and S. A. Malik, *J. Inorg. Nucl. Chem.*, 1967, **29**, 2935–2944.
- 38 C. M. Tourné, G. F. Tourné, S. A. Malik and T. J. R. Weakley, *J. Inorg. Nucl. Chem.*, 1970, **32**, 3875–3890.
- 39 C. Rocchiccioli-Deltcheff, M. Fournier, R. Franck and R. Thouvenot, *Inorg. Chem.*, 1983, **22**, 207–216.
- 40 M. S. Balula, J. A. Gamelas, H. M. Carapuça, A. M. V. Cavaleiro and W. Schlindwein, *Eur. J. Inorg. Chem.*, 2004, 619–628.
- 41 T. Kottke and D. Stalke, *J. Appl. Crystallogr.*, 1993, **26**, 615–619.
- 42 APEX2, *Data Collection Software Version 2.1-RC13*, Bruker AXS, Delft, The Netherlands, 2006.
- 43 Cryopad, *Remote monitoring and control, Version 1.451*, Oxford Cryosystems, Oxford, United Kingdom, 2006.
- 44 SAINT+, *Data Integration Engine v. 7.23a*©, 1997–2005, Bruker AXS, Madison, Wisconsin, USA.
- 45 G. M. Sheldrick, *SADABS v.2.01, Bruker/Siemens Area Detector Absorption Correction Program*, 1998, Bruker AXS, Madison, Wisconsin, USA.
- 46 G. M. Sheldrick, *Acta Crystallogr., Sect. A: Found. Crystallogr.*, 2008, **64**, 112–122.
- 47 G. M. Sheldrick, *SHELXS-97, Program for Crystal Structure Solution*, University of Göttingen, 1997.
- 48 G. M. Sheldrick, *SHELXL-97, Program for Crystal Structure Refinement*, University of Göttingen, 1997.
- 49 M. Choi, F. Kleitz, D. N. Liu, H. Y. Lee, W. S. Ahn and R. Ryoo, *J. Am. Chem. Soc.*, 2005, **127**, 1924–1932.
- 50 C. Pereira, K. Biernacki, S. L. H. Rebelo, A. L. Magalhaes, A. P. Carvalho, J. Pires and C. Freire, *J. Mol. Catal. A: Chem.*, 2009, **312**, 53–64.
- 51 R. R. L. Martins, M. Neves, A. J. D. Silvestre, A. M. S. Silva and J. A. S. Cavaleiro, *J. Mol. Catal. A: Chem.*, 1999, **137**, 41–47.
- 52 R. R. L. Martins, M. Neves, A. J. D. Silvestre, M. M. Q. Simoes, A. M. S. Silva, A. C. Tome, J. A. S. Cavaleiro, P. Tagliatesta and C. Crestini, *J. Mol. Catal. A: Chem.*, 2001, **172**, 33–42.
- 53 M. S. S. Balula, I. C. M. S. Santos, J. A. F. Gamelas, A. M. V. Cavaleiro, N. Binsted and W. Schlindwein, *Eur. J. Inorg. Chem.*, 2007, 1027–1038.
- 54 S. Y. Yu, J. X. Lu, Y. K. Shan, M. Y. He and L. Y. Dai, *Z. Kristallogr. - New Cryst. Struct.*, 2002, **217**, 449–450.
- 55 L. Y. Dai, Y. K. Shan and M. Y. He, *J. Mol. Struct.*, 2003, **644**, 165–170.

- 56 C. M. Tourne and G. Tourne, *C. R. Seances Acad. Sci., Ser. C*, 1968, **266**, 1363–1365.
- 57 J. Visser, ICDD Grant-in-Aid, 1992.
- 58 B. J. S. Johnson and A. Stein, *Inorg. Chem.*, 2001, **40**, 801–808.
- 59 Y. H. Guo, C. W. Hu, C. J. Jiang, Y. Yang, S. C. Jiang, X. L. Li and E. B. Wang, *J. Catal.*, 2003, **217**, 141–151.
- 60 V. N. Panchenko, I. Borbath, M. N. Timofeeva and S. Gobolos, *J. Mol. Catal. A: Chem.*, 2010, **319**, 119–125.
- 61 C. H. Chiang, H. Ishida and J. L. Koenig, *J. Colloid Interface Sci.*, 1980, **74**, 396–404.
- 62 C. Rocchiccioli-Deltcheff and R. Thouvenot, *J. Chem. Res., Synop.*, 1977, 46.
- 63 K. Nomiya, Y. Sugie, K. Amimoto and M. Miwa, *Polyhedron*, 1987, **6**, 519–524.
- 64 C. Yu, B. Tian, X. Liu, J. Fan and H. Yang, *Advances in Mesoporous Materials Templated by Nonionic Block Copolymers*, Imperial College Press, London, 2004.
- 65 M. Kruk, M. Jaroniec, C. H. Ko and R. Ryoo, *Chem. Mater.*, 2000, **12**, 1961–1968.
- 66 K. S. W. Sing, D. H. Everett, R. A. W. Haul, L. Moscou, R. A. Pierotti, J. Rouquerol and T. Siemieniewska, *Pure Appl. Chem.*, 1985, **57**, 603–619.
- 67 J. L. C. Sousa, I. Santos, M. M. Q. Simoes, J. A. S. Cavaleiro, H. I. S. Nogueira and A. M. V. Cavaleiro, *Catal. Commun.*, 2011, **12**, 459–463.
- 68 I. Santos, M. M. Q. Simoes, M. Pereira, R. R. L. Martins, M. Neves, J. A. S. Cavaleiro and A. M. V. Cavaleiro, *J. Mol. Catal. A: Chem.*, 2003, **195**, 253–262.
- 69 I. Santo, S. L. H. Rebelo, M. S. S. Balula, R. R. L. Martins, M. Pereira, M. M. Q. Simoes, M. Neves, J. A. S. Cavaleiro and A. M. V. Cavaleiro, *J. Mol. Catal. A: Chem.*, 2005, **231**, 35–45.
- 70 A. C. Estrada, M. M. Q. Simoes, I. Santos, M. Neves, J. A. S. Cavaleiro and A. M. V. Cavaleiro, *Monatsh. Chem.*, 2010, **141**, 1223–1235.
- 71 E. Poli, R. De Sousa, F. Jerome, Y. Pouilloux and J. M. Clacens, *Catal. Sci. Technol.*, 2012, **2**, 910–914.
- 72 P. A. Shringarpure and A. Patel, *React. Kinet., Mech. Catal.*, 2011, **103**, 165–180.
- 73 J. Tang, X. L. Yang, X. W. Zhang, M. Wang and C. D. Wu, *Dalton Trans.*, 2010, **39**, 3396–3399.
- 74 M. R. Maurya, P. Saini, C. Haldar and F. Avecilla, *Polyhedron*, 2012, **31**, 710–720.
- 75 T. Punniyamurthy, S. Velusamy and J. Iqbal, *Chem. Rev.*, 2005, **105**, 2329–2363.
- 76 Y. Yang, Y. Zhang, S. J. Hao and Q. B. Kan, *Chem. Eng. J.*, 2011, **171**, 1356–1366.
- 77 M. J. Beier, W. Kleist, M. T. Wharmby, R. Kissner, B. Kimmerle, P. A. Wright, J. D. Grunwaldt and A. Baiker, *Chem.-Eur. J.*, 2012, **18**, 887–898.
- 78 B. Tamami and S. Ghasemi, *Appl. Catal., A*, 2011, **393**, 242–250.
- 79 P. Shringarpure, K. Patel and A. Patel, *J. Cluster Sci.*, 2011, **22**, 587–601.
- 80 P. Zhang, M. Yang and X. P. Lu, *Asian J. Chem.*, 2007, **19**, 2083–2092.
- 81 A. J. Stapleton, M. E. Sloan, N. J. Napper and R. C. Burns, *Dalton Trans.*, 2009, 9603–9615.